PAGE FORMATTING:

Page Layout: Portrait
Page header: 2016 AETC
Margins: 0.7" (all –top, bottom, left and right)

TEXT FORMATTING:

ID: 703

Digital Expert for DAS Passive Seismic Monitoring: Integration of Image Processing and Geophysical Processing

Takashi Mizuno, Joel Le Calvez, Nicholas Fundytus, and Pierre Bettinelli (SLB)

ABSTRACT

Space

Passive seismic monitoring using 3C sensors is a domain where real-time delivery has been commercially implemented for the last several decades. DAS-acquired datasets pose a challenge to real-time delivery of hypocenters due to (i) the large data volumes involved (order of 2 to 4 compared to conventional acquisition methods) and (ii) relatively low signal-to-noise ratio data. We present a new real-time processing flow that involves image processing techniques applied to induced seismic datasets. Our approach mimics the expert geophysicist's view to identify passive seismic events acquired using DAS data leveraging an algorithm integrating both image processing and traditional geophysical processing.

EXTENDED ABSTRACT

Introduction

Passive seismic monitoring has been used for hydraulic fracturing monitoring in tight and unconventional reservoirs (e.g., Warpinski et al. 1998a; Warpinski et al., 1998b) as well as for geothermal energy development (e.g., Jones et al., 1995) among many other applications. Most of the time, a single monitoring array deployed downhole is considered to be the best option compromising data quality, cost and operational considerations. To this end, over the last decades, wireline-deployed 3C geophone systems have generally been used. Distributed Acoustic Sensing (DAS) is now capable of microseismic monitoring (e.g., Webster et al. 2013; Karrenbach et al. 2017; Molteni et al. 2017) using optical fiber logging technology. However, DAS-acquired datasets are challenging when it comes to real-time delivery of processed hypocenters and associated source parameters due to the large data volumes involved (order of 2 – 4 compared to conventional methods) and relatively low (signal-to-noise ratio (SNR).

The fundamental requirements of passive seismic monitoring are (1) to identify the passive seismic signals from continuous ground motion data, (2) to locate each detected microseismic event, and (3) to estimate the magnitude of each mapped event. In the present study, we focus on the first two steps: (1) event detection and (2) hypocenter determination from continuous data as estimating magnitude requires those first two steps to be completed.
Figure 1 is a summary of technologies that have been used in relation to this study. Historically the problem has been dealt with by the geophysics-model-driven approach to seismic data. The travel-time-based methods (Geiger's method; e.g., Geiger, 1912), characteristic function-based (migration-based; e.g. Kao and Shan, 2004; Gharti et al., 2010; Drew et al., 2005) methods, and full-waveform-based methods (e.g., Jarillo Michel and Tsuvankin, 2014a and 2014b) are categorized into that group. In the case of the Geiger's method, an expert geophysicist reads the signal arrival either or both P and S wavesfrom continuous waveform data and runs the algorithm to fit the arrival of P and S waves by revising the hypocenter. The other two methods use seismic waveforms instead to obtain the hypocenter. To apply those methods to DAS-acquired data, we need to scale up the computation in order to handle the large data volume. The second approach is machine learning (ML), in which we first train the algorithm to obtain the relation between seismic data and model parameters (i.e., hypocenter). Then we apply the algorithm to the dataset. The training process is vital since it is the only process to embed the geophysical relation between data and model parameters since the algorithm is not backed by any type of geophysical forward modeling. We need to enhance the training process to handle a large amount of DAS data which includes preparation of training dataset as well as training the algorithm. The first two approaches need to handle large amount of data when it comes to computation. We present the third approach, in which an "image file of seismic data" is used instead of a large volume of seismic data. Since seismic data is "regularized" during the conversion to image data, we anticipate the event location is still invertible, although the size of the data is reduced. Applied to passive seismic monitoring for example, the algorithm identifies P and/or S arrivals from the image data, and then estimates the event location for each file. This is a digital model of what an expert geophysicist is doing by looking at seismic data on a typical display at the well site.

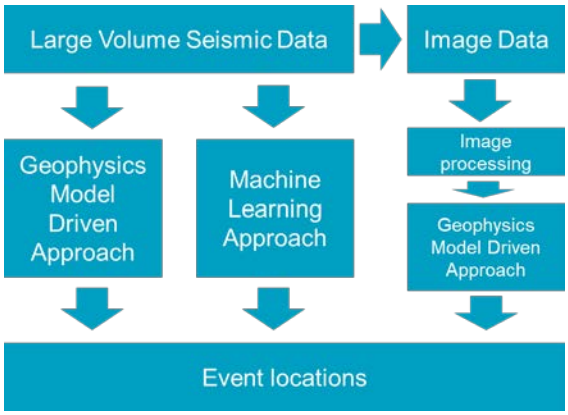

Figure 1: Input and output of three different approaches to address the event location problem. We studied the geophysics model-driven approach for image data generated by a large volume of seismic data.

Passive Seismic Processing Using Image Data File

Figure 2 presents the overall processing flow from seismic data files to event locations. The algorithm performs the arrival time-picking followed by the hypocenter determination. This is comparable to a conventional passive seismic processing. However, the details are different from mimicking the steps an expert geophysicist is performing.

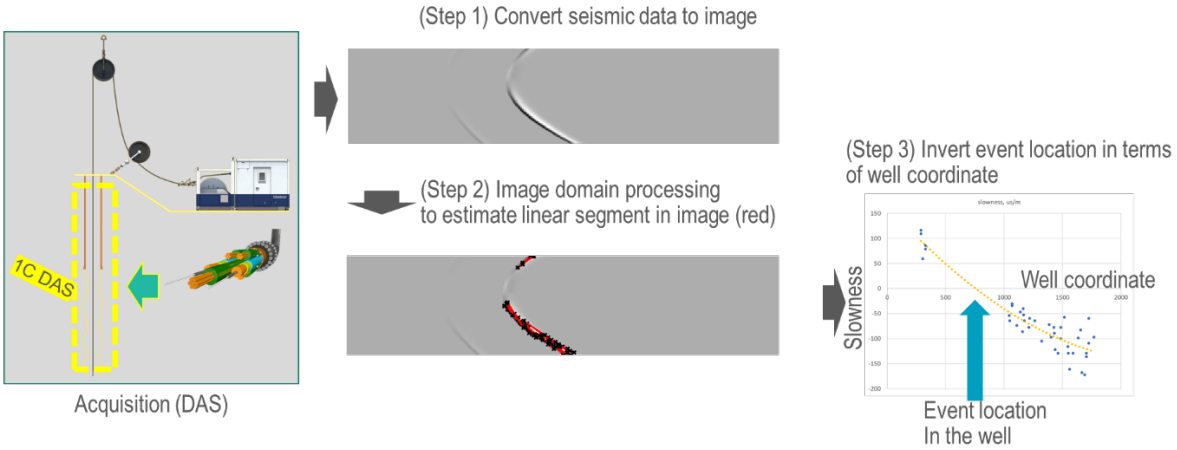

Figure 2: High-level description of the processing of passively-acquired microseismic data from event detection to hypocenter determination using image data. First seismic data are converted to a black and white image. It is followed by an image processing, including edge detection and Hough transform to identify a series of linear segments as seismic phase arrivals. The slope of the linear segments is analyzed in terms of distance along the fiber, and

the location of the event is estimated in terms of the depth of the fiber. This is performed in real-time since data size is significantly reduced. Furthermore, there is no need for velocity data since this method solves event location in terms of the depth of the fiber, not distance from the fiber.

In conventional geophysical processing, automated time-picking relies on signal-to-noise ratio or other statistical measures of the seismic waveform considering the trace-by-trace approach. This is applicable to sparse seismic arrays. In the image-domain geophysics processing, the algorithm looks at the "edge" of the seismic image data, which corresponds to the coherent arrival of seismic energy at several neighboring receivers (Figure 2). Firstly, we convert the seismic data to a black and white image file (Figure 3). This conversion reduces the overall volume of information to be considered for processing. Secondly, we perform (a) an edge detection to enhance the seismic signal, and (b) a Hough transform to identify seismic arrivals. This is to imitate what the domain specialists are doing during the traditional seismic data QC steps in the field. The Hough transform also elucidates non-seismic features (local cable noises and borehole modes traveling along the borehole). Subsequently, we perform some trimming using *a priori* geophysics information. This is also another imitation of what the domain expert performs unconsciously. Once all necessary seismic information has been provided, we use geophysical inversion method to infer microseismic events and time applicable to the image domain in the next step.

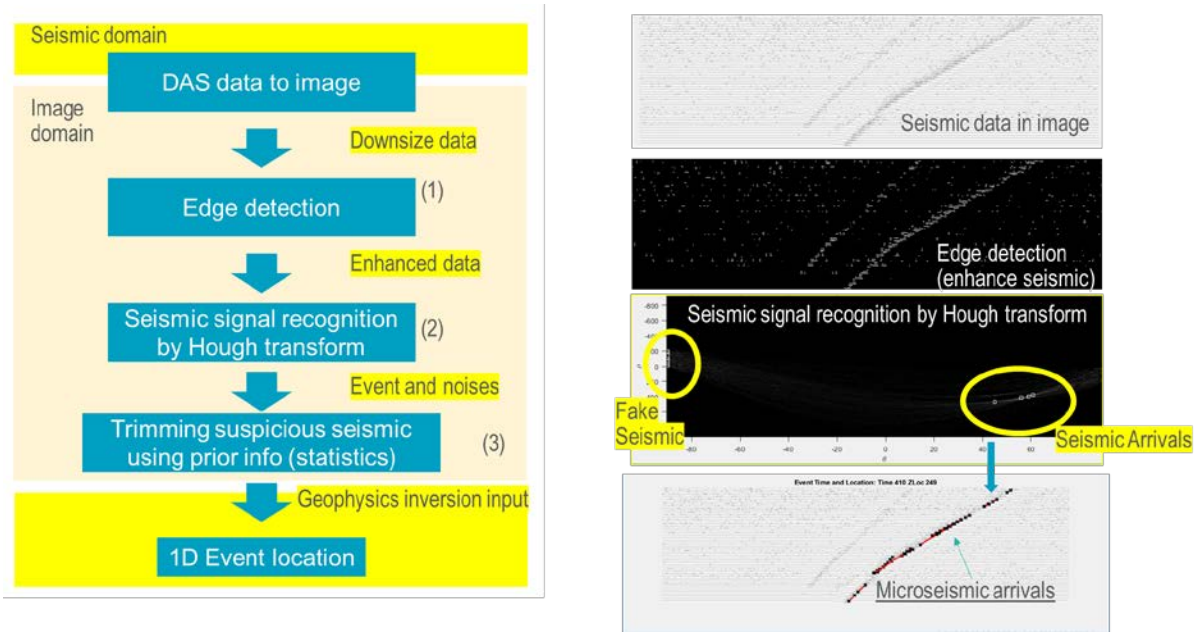

Figure 3: Processing flow of phase arrival detection for an image file of seismic data. First, we generate a seismic image file from continuous seismic data by time windowing. Either seismic wiggle or density plot is possible. Then we perform an edge detection of the seismic image data by thresholding the image file and computing the derivative in space. This leads

to an enhanced view of the seismic image data in terms of phase arrivals. To analyze the slope of the phase arrivals, we used the Hough transform. We obtain the amplitude of the edge image in the slope and intercept domain, which is similar of the Tau-p transform in traditional seismic data processing. After applying filters to the Hough transform result to eliminate non-seismic arrivals, we are able to obtain seismic arrivals in the image domain. Please note coherent noise can be isolated from seismic signals by Hough transform (marked in yellow circle in right).

As an option of the geophysics inversion method, Geiger's location algorithm could be applicable because we can obtain the arrivals time of seismic phases from the slope located by the previous step. However, we need to note that image processing detects slope rather than travel times. Also the image process does not enable labeling either the P or S waves for the slope. Considering the fact that the expert geophysics carry on event location by looking at variation of the slope of arrival without the phase labeling and velocity model, , we developed its digital representation of an expert geophysicist in the field. The method uses the slope as the data and do not rely on labeling of P and S waves and velocity model. We look at the distribution of the slope of arrivals of the image file (Figure 2), instead of the arrival time at each station. Figure 4 shows the relation between the distribution of slope parameters and receiver depth along the fiber. In this example, the event occurred at depth = 0, while the distance to the fiber is changed from 100 m to 500 m. The slope is presented as slowness, which is the inverse of velocity estimated from the image data. If the slope is vertical in the image domain, the slowness corresponds to zero. If the slope is gentle, the absolute value of the slope increases. As shown, no matter the distance of the event to the fiber, the polarity of slowness changes at the event depth. This means we can invert the depth of the event by looking at the zero-crossing point in the slowness distribution. The above nature of polarity changes in slowness can be seen even if slope data contains for both P and S and not labelled. Figure 5 is an example of slowness – depth variation for an event occurring at a depth of 150 m and a distance of 200 m to the fiber. Zero-crossing of P and S was observed at a depth of 150 m, which corresponds to the depth of the event. To invert this depth, we apply a polynomial curve fitting to the unlabeled slope distribution datasets. Although the dataset contains both P and S, polynomial curve fitting explains the distribution of the slowness data with depth of event of 150 m.. We are able to invert the depth of events relying solely on the slope information deduced from the image data file as the linear inversion of the polynomial.

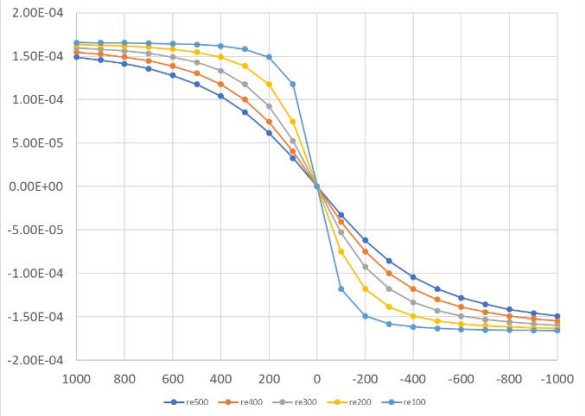

Figure 4: The slowness (vertical axis) and its variation with the receiver position (horizontal axis) in the monitoring well. The event is located at a depth of 0 m. Although the shape of the curve changes with the distance of the event to the well (r_e), each shows a zero-crossing at the depth of 0 m where the event is located.

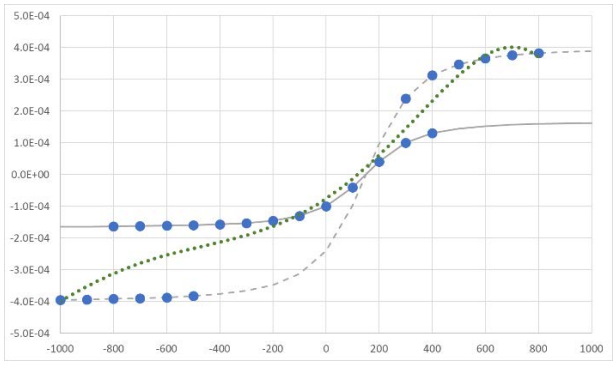

Figure 5: (Blue) The slowness (converted from the slope in the image) in case the event occurs at a depth of 150 m and its distance to the array is 200 m. Two series of slope distributions are merged: one (on dotted silver lines) is for the S-wave, and the other (on solid silver line) is for the P-wave, assuming image processing could not label the arrival of seismic phases. The dotted green line is the result of the linear fitting of a 5th order polynomial. The intercept of the zero-crossing of the polynomial curve (dotted green line) is close to the true zero-crossings of the solid silver line and the dotted silver line. The depth of the event can be inferred by the distribution of the unlabeled slope information using polynomial curve fitting.

We apply the technology to a 15-minute-long dataset for more than 1,200 DAS channels. Figure 6 shows the example of phase detection. The algorithm captures the changes of slope along the depth of the fiber optics cable as expected in Figures 4 and 5. Over the 15-minute-long time interval sampled, we detected over 30 microseismic events located automatically (Figure 6). We also observed that different types of edge detection technologies and different image resolution yield different performances. The processing can be performed in 10 minutes on a typical laptop, which indicates real time processing is possible. We can speed up the afore mentioned processing approach by using a high-performance computing machine at the well site. We conclude that image processing is a reasonable alternative for the processing of passive seismic monitoring.

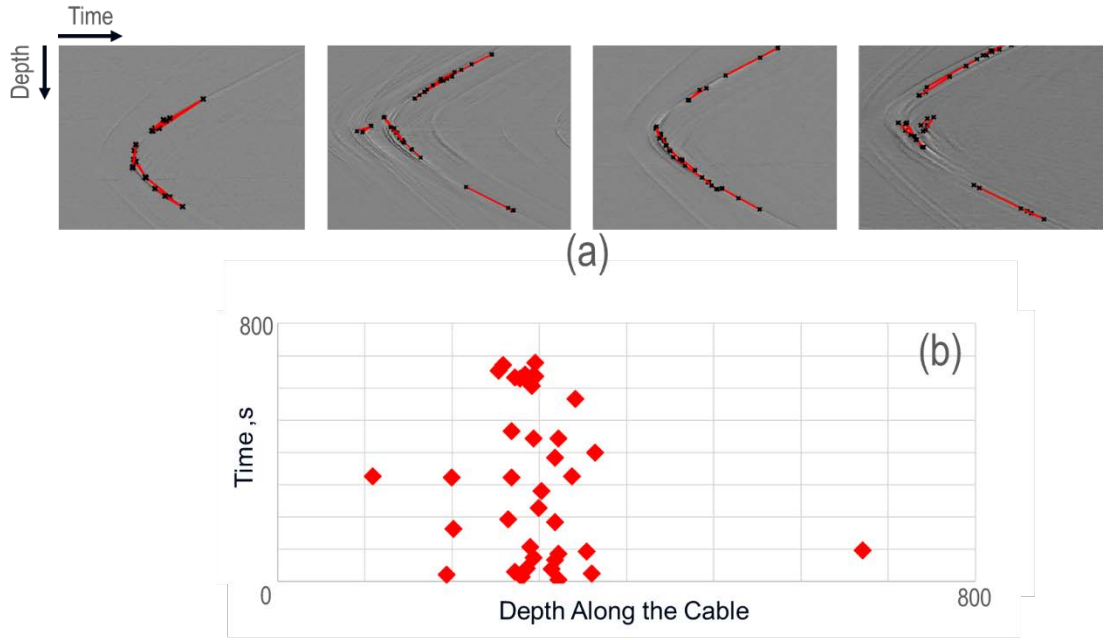

Figure 6: Example of optical fiber-recorded passive seismic data processed in the image domain. (a) Four examples of images of seismic data (black and white) and phase detection using Hough transform (red). (b) Cross-plot of event depth vs. time. Events are occurring at a certain depth matching the one from the image domain (a).

Discussion and Conclusion

Considering the fact that the final processing QC is done by expert geophysicists relying on their eyes using a display, which is far less than the original volume of DAS seismic data, data processing in the image domain is a viable alternative to traditional approaches. In the present study, we propose one form of digital replacement. In the real data example, the size of the data is reduced by 80 % and more using the tiff file. The image file has been used as just a thumbnail of seismic data in the database. However, we anticipate the research of

image file format in terms of the capability of processing since the capability of the processing could be limited by the choice of an image file.

The Hough transform can be applicable for other than passive seismic processing since the majority of geophysics processing focuses on a measure of seismic arrivals. It will be applicable to tomography and imaging problem. This is a great advantage for real-time time-lapse processing. However, it is not applicable to problems requiring absolute amplitude modeling since we employ rescaling and normalization of data when image datasets generated from seismic dataset.

Image data are often discussed in conjunction with the application of machine learning technology to geophysics datasets. However, this case study demonstrates the great potential brought by the integration of image domain processing and traditional processing of geophysical data for real-time delivery of DAS-acquired datasets thanks to the redundancy of information present in DAS-acquired data.

Acknowledgment

We appreciate XXX to share us the data for our study and approve the publication. We thank SLB colleagues for continuous support for the project.

References

1. Bazalgette, L., Salim, H., 2018, Mesozoic and Cenozoic structural evolution of North Oman, new insight from high-quality 3D seismic from the Lekhwair area, Journal of structural geology.
2. Drew, J., Leslie, D., Armstrong, P., and Michaud, G. (2005). *Automated microseismic event detection and location by continuous spatial mapping*. Paper SPE-5513-MS presented at the SPE Annual Technical Conference and Exhibition, Dallas, Texas. https://doi.org/10.2118/95513-MS.
3. Gharti, H. N., Oye, V., Roth, M., and Kuehn, D. (2010). Automated microearthquake location using envelope stacking and robust global optimization. *Geophysics*, 75, MA 27 – MA 46. https://doi.org/10.1190/1.3432784
4. Geiger, L. (1912). Probability method for the determination of earthquake epicenters from the arrival time only. *Bulletin of St. Louis University*, 8, 60–71.
5. Jarillo Michel, O., and Tsvankin, I. (2014a). Gradient calculation for waveform inversion of microseismic data in VTI media. *Journal of Seismic Exploration*, 23, 201–217.
6. Jarillo Michel, O., and Tsuvankin, I. (2014b). Waveform inversion for parameters of microseismic sources in VTI media. *SEG Technical Program Expanded Abstracts 2014*, 1045 – 1048. https://doi.org/10.1190/segam2018-2990944.1
7. Kao, H., and Shan, S. J. (2004). The source-scanning algorithm: mapping the distribution of seismic sources in time and space. *Geophysical Journal International*, 157, 589–594. https://doi.org/10.1111/j.1365-246x.2004.02276.x
8. Karrenbach M., Ridge, A., Cole, S., Boone, K., Kahn, D., Rich, J., Silver, K., and Langton, D. (2017). DAS microseismic monitoring and integration with strain measurement in hydraulic fracture profiling. Presented at the Unconventional Resource Technology Conference, Austin, Texas. https://doi.org/10.15530/URTEC-2017-2670716.
9. Molteni, D., Williams, M. J., and Wilson, C. (2017). Detecting microseismicity using distributed vibration. *First Break*, 35, 51–55.

10. Warpinski, N. R., Branagan, P. T., Peterson, R. E., and Wolhart, S. L. (1998). *An interpretation of M-Site hydraulic fracture diagnostic results*. Paper SPE-39950-MS presented at the SPE Rocky Mountain Regional/Low Permeability Reservoirs Symposium, Denver, Colorado. https://doi.org/10.2118/39950-MS
11. Warpinski, N. R., Branagan, P. T., Peterson, R. E., Wolhart, S. L., and Uhl, J. E. (1998). *Mapping hydraulic fracture growth and geometry using microseismic events detected by a wireline retrievable accelerometer array*. Paper SPE-40014-MS presented at the SPE Gas Technology Symposium, Calgary, Alberta. https://doi.org/10.2118/40014-MS
12. Webster, P., Wall, J., Perkins, C., and Molenaar, M. (2013). Micro-seismic detection using distributed acoustic sensing. *SEG Technical Program Expanded Abstracts 2013*, 2459 – 2463. https://doi.org/10.1190/segam2013-0182.1